Gaussian setting time for solute transport in fluvial systems

Yong Zhang[1] and Mark M. Meerschaert[2]

Received 8 October 2010; revised 27 May 2011; accepted 13 June 2011; published 3 August 2011.

[1] Gaussian setting time is the time scale at which solute plumes converge to their asymptotic Gaussian shape. This study estimates the Gaussian setting time using a high-resolution hydrofacies model of a typical fluvial system, with an instantaneous point source in the mobile phase. Monte Carlo simulations are augmented by a time-nonlocal transport model to forecast plume shape at late time. Analysis of plume spatial moments indicates that convergence to Fickian transport is affected by molecular diffusion and the thickness of low-permeability floodplain layers. These layers can cause non-Gaussian tailing to persist at late time because the low-permeability lenses are elongated in the horizontal, so that most particles escape vertically by diffusion. A simple empirical setting time formula is developed, which can be fitted using data from driller's logs that characterize the thickness of the low-permeability lenses. The empirical formula may be useful for predicting setting time in fluvial aquifers similar to those considered in this study. For such aquifers, the plume will often exit the region prior to the setting time, so the asymptotic Gaussian model will not be a useful predictor of plume shape.

Citation: Zhang, Y., and M. M. Meerschaert (2011), Gaussian setting time for solute transport in fluvial systems, *Water Resour. Res.*, *47*, W08601, doi:10.1029/2010WR010102.

1. Introduction

[2] Traditional theory holds that passive tracer transport through stationary heterogeneous media should converge to Gaussian limits after sampling all scales of heterogeneity. The transition from non-Fickian transport to asymptotic limits is a fundamental issue in stochastic hydrology [*Dagan and Fiori*, 2003]. Of particular interest is the Gaussian setting time t_S required to reach Gaussianity. This value is important in assessing long-term water quality, and understanding the transient non-Fickian diffusion observed in many geophysical processes [*Meerschaert et al.*, 2008]. Prediction of t_S however is complicated by the intrinsic complexity of natural geological formations.

[3] This study develops a convenient formula for the Gaussian setting time t_S that is valid for transport in regional-scale fluvial aquifer-aquitard systems, assuming a point source in the mobile phase. Section 2 develops a realistic Monte Carlo transport model, taking into account the influence of medium heterogeneity (characterized by driller's logs) and tracer diffusivity. Since it is not practical to run the Monte Carlo model over very long time scales, section 3 fits the Monte Carlo results to a stochastic model. Then section 4 computes the Gaussian setting time t_S by checking convergence of plume spatial moments up to fourth order. Two end-member scenarios are presented as an example of the extensive simulations conducted to develop and verify the setting time formula (7). This formula provides a practical method for determining the travel time needed before tracer plumes become approximately Gaussian. It also indicates those situations where Gaussian convergence cannot be expected because the plume exits the region before the setting time.

2. Monte Carlo Simulations

[4] Monte Carlo simulations conducted by *Zhang et al.* [2007] and *LaBolle and Fogg* [2001] showed that passive tracer transport in a fine-material-dominated fluvial system, such as the one underlying the Lawrence Livermore National Laboratory site, exhibits transient non-Fickian behavior. The simulated late time tail of breakthrough curve (BTC) transforms from power law to exponential because of the finite thickness of diffusion-limited clayey material (i.e., floodplain deposits). In this section, we extend the above two studies by also considering coarse-material-dominated systems, and evaluating the influence of molecular diffusion on the setting time, as suggested by *Fiori et al.* [2003].

[5] Here we introduce the Monte Carlo approach briefly. Details are given by *LaBolle and Fogg* [2001]. A Markov Chain indicator model [*Carle and Fogg*, 1996] generates high-resolution realizations of hydrofacies architecture (given driller's logs; see Figure 1a). Then steady state discharge vectors are calculated for these hydrofacies models, and finally, solute transport is simulated using the code RWHet [*LaBolle*, 2006]. Model parameters, boundary conditions, and tracer injection mode are the same as those used by *Zhang et al.* [2007]. In particular, the hydrodynamic dispersion coefficient is the sum of mechanical dispersion (with an isotropic dispersivity 0.01 m, as suggested by *LaBolle and Fogg* [2001]) and molecular diffusion ($D^\star$). An instantaneous point source was used.

[1]Division of Hydrologic Sciences, Desert Research Institute, Las Vegas, Nevada, USA.
[2]Department of Statistics and Probability, Michigan State University, East Lansing, Michigan, USA.

0043-1397/11/2010WR010102

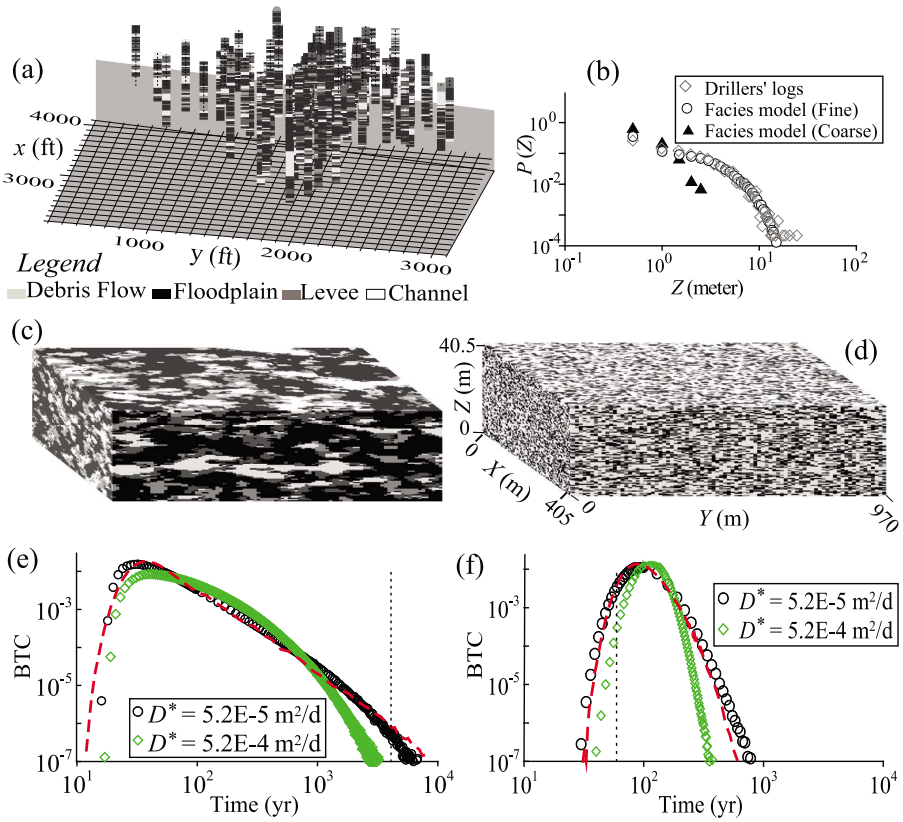

Figure 1. (a) Driller's logs at the Lawrence Livermore National Laboratory site. (b) Probability density function for thickness of floodplain layers, denoted as $P(Z)$. Three-dimensional view of the hydrofacies model for (c) Scenario-Fine and (d) Scenario-Coarse. Breakthrough curve at L = 400 m for (e) Scenario-Fine and (f) Scenario-Coarse. The long-dashed line in Figures 1e and 1f denotes the model simulation, and the vertical dashed lines indicate the diffusion time scale $t = 1/\lambda$.

[6] In a typical fluvial system, low-permeability floodplain deposits form the relatively immobile layers, while highly permeable nonfloodplain deposits compose the interconnected mobile phase [*LaBolle and Fogg*, 2001]. In the following, we term the fine-material-dominated system "Scenario-Fine" (Figure 1c), and the coarse-grain system "Scenario-Coarse" (Figure 1d). Each scenario produced 100 realizations, whose average provides the ensemble plume BTCs shown in Figures 1e and 1f.

[7] Monte Carlo simulations of BTCs show that both the low-permeability deposits and the tracer diffusivity affect the convergence to Fickian transport by controlling the residence time of solute particles. Firstly, the thickness distribution of flood plain layers (denoted as $P(Z)$) affects residence times for solute particles. A combination of broader residence times (due to a wider distribution of floodplain layers with different thickness) produces a heavier trailing edge, and a longer setting time t_S. For example, the BTC tail for Scenario-Fine (Figure 1e) is obviously heavier than that for Scenario-Coarse (Figure 1f) with a narrower $P(Z)$ (Figure 1b). Secondly, the molecular diffusion of the tracer governs the residence time for a given floodplain layer. An increase of D^* can decrease residence time and accelerate the transition from non-Fickian to Fickian diffusion, resulting in a faster setting time (Figures 1e and 1f). The dominant effect of molecular diffusion on late time tracer dynamics is consistent with the traditional multirate mass transfer (MRMT) process: the mobile part of the plume washes away first, and the late time tail is composed of immobile particles leaking out into the mobile zone.

3. Stochastic Model

[8] Since it is not practical to run the Monte Carlo model from section 2 over very long time scales, here we develop a stochastic model to extrapolate tracer transport over the time scale needed to assess Gaussian convergence. The tempered stable Lévy motion (TSLM) model developed by *Meerschaert et al.* [2008] describes a two-phase transient anomalous dispersion process that is asymptotically Gaussian:

$$\frac{\partial C_M}{\partial t} + \beta \frac{\partial^{\gamma,\lambda}}{\partial t} C_M = -V \frac{\partial C_M}{\partial x} + D \frac{\partial^2 C_M}{\partial x^2} - C_{M,0} \beta g(t) \qquad (1a)$$

$$\frac{\partial C_T}{\partial t} + \beta \frac{\partial^{\gamma,\lambda}}{\partial t} C_T = -V \frac{\partial C_T}{\partial x} + D \frac{\partial^2 C_T}{\partial x^2}, \qquad (1b)$$

where C_M and C_T $[ML^{-3}]$ denote the dissolved solute concentrations in the mobile and total (mobile plus immobile) phases, respectively, γ (dimensionless) is the order of the time

fractional derivative, β $[T^{\gamma-1}]$ is the fractional capacity coefficient, λ $[T^{-1}]$ is the tempering strength, V $[LT^{-1}]$ denotes velocity, D $[L^2\ T^{-1}]$ dispersion strength, $C_{M,0}$ the initial concentration, $g(t) = -\int_t^\infty e^{-\lambda\tau}\tau^{-\gamma-1}/\Gamma(-\gamma)d\tau$ $[T^{-\gamma}]$ the memory function (Γ is the gamma function), and $\partial^{\gamma,\lambda}/\partial t$ denotes the tempered fractional derivative. This model is a special case of the MRMT [cf. *Willmann et al.*, 2008], with an exponentially tempered power law memory function that represents the combination of immobile zones with different thickness. It is conceptually similar to a CTRW with truncated or tempered power law waiting times [*Dentz et al.*, 2004; *Bijeljic and Blunt*, 2006] but has the advantage that the underlying differential equations can be specified. The use of tempered stable retention times in hydrology was originally suggested by *Cvetkovic and Haggerty* [2002]. The power law index γ indicates the range of thickness, with a smaller γ indicating a wider range. The parameter λ, related to the classical diffusion characteristic time, accounts for the influence of molecular diffusion and floodplain thickness on tracer dynamics:

$$\lambda = D^*/(Z^*)^2 \tag{2}$$

where Z^* $[L]$ represents the effective thickness of floodplain layers. *Zhang et al.* [2007] found that residence time in a thickness-averaged floodplain layer is a good approximation to the transition time of BTC slopes. Hence we take Z^* simply as the average thickness.

[9] Formula (2) was used to estimate λ on the basis of the BTCs obtained from Monte Carlo simulations in section 2. Both λ and the velocity V can be predicted (V is estimated as the arithmetic mean). The predicted λ using (2) is 1.687×10^{-2} yr^{-1} for Scenario-Coarse and 2.450×10^{-4} yr^{-1} for Scenario-Fine, and V is 12.15 and 14.64 m/yr for Scenario-Coarse and Scenario-Fine, respectively. The remaining parameters are obtained by fitting the BTC (Figures 1e and 1f). The best fit parameters are $\gamma = 0.69$, $\beta = 0.98$ yr$^{-0.31}$, and $D = 45$ m^2/yr for Scenario-Coarse, and $\gamma = 0.59$, $\beta = 0.28$ yr$^{-0.41}$, and $D = 140$ m^2/yr for Scenario-Fine. The general match between Monte Carlo and TSLM simulations shows the applicability of TSLM and (2). We also used TSLM to predict BTCs at various locations, and tracer snapshots at various times, which generally match the Monte Carlos simulations (not shown), to further validate the stochastic model.

[10] The truncation parameter λ controls the transition from power law distribution to exponential for the late time BTC [*Meerschaert et al.*, 2008]. When time $t \gg 1/\lambda$, non-Fickian transport converges gradually to Fickian, leading to the well-known estimate [*Attinger et al.*, 1999] for Gaussian setting time

$$t_S \gg 1/\lambda = (Z^*)^2/D^*. \tag{3}$$

This formula will be tested and refined in section 4.

4. Setting Time via Plume Spatial Moments

[11] To estimate Gaussian setting time t_S and refine (3), we explore the temporal evolution of plume spatial moments. First we analytically compute the asymptotic moments of the TSLM model (1), and then we apply the results of section 3 to determine the travel time t_S required for the simulated plume moments to approach their asymptotic values.

4.1. Asymptotic Moments for Gaussian Limits

[12] Asymptotic moments are first derived for the total phase, model (1b). The nth-order moment $v_T^n(s)$ in Laplace space $t \mapsto s$ are $v_T^n(s) = i^n d^n C_T(k, s)/dk^n|_{k=0}$, where $C_T(k, s)$ is the solution of (1b) in Fourier ($x \mapsto k$) and Laplace space. The late time approximation of $v_T^n(t)$ is obtained by the inverting the Laplace transform of v_T^n ($s \to 0$). The resulting late time asymptotic moments up to fourth order, including the mass (M_T), mean (E_T), variance (σ_T^2), skewness (S_T), and kurtosis (κ_T), take the form:

$$M_T = 1, \tag{4a}$$

$$E_T \approx \frac{Vt}{1+\beta\gamma\lambda^{\gamma-1}}, \tag{4b}$$

$$\sigma_T^2 \approx \frac{2Dt}{1+\beta\gamma\lambda^{\gamma-1}} + \frac{\beta\gamma(1-\gamma)\lambda^{\gamma-2}V^2t}{(1+\beta\gamma\lambda^{\gamma-1})^3}, \tag{4c}$$

$$S_T \approx \frac{\frac{9}{4}b^2V^3 - 6bVD}{a^{1/2}(2D-bV^2)^{3/2}}t^{-1/2} \to 0, \tag{4d}$$

$$\kappa_T \approx \frac{-3b^3V^4 + 42b^2V^2D - 24bD^2}{a(2D-bV^2)^2}t^{-1} \to 0, \tag{4e}$$

where "$_T$" denotes the total phase, $a = 1/(1+\beta\gamma\lambda\gamma^{-1})$, and $b = a^2\beta(\gamma-1)\gamma\lambda^{\gamma-2}$.

[13] The late time spatial moments in the mobile phase (1a) are the same as (4), except for the decline of mobile mass

$$M_M \approx 1/\left(1+\beta\gamma\lambda^{\gamma-1}\right). \tag{5}$$

[14] The asymptotes (4) show that both mean and variance increase linearly with time. Skewness and kurtosis tend to zero, but κ_T falls to zero faster than S_T. The same pattern was observed by *Fiori et al.* [2003] for a multi-indictor model of permeability structure.

[15] The setting time t_S can be estimated given the asymptotic skewness (4d). Using $|S| \le 0.04$ as the criterion for skewness to approach zero, we obtain the setting time

$$t_S = \left[\frac{a^{1/2}(2D-bV^2)^{3/2}}{56.25b^2V^3 - 150bVD}\right]^{-2}. \tag{6}$$

The threshold $|S| \le 0.04$ is similar to the one used by *Fiori et al.* [2003], and the resulting values of t_S give reasonable results for every scenario simulated, two of which are included in this paper. This setting time formula (6) can be calculated only after model parameters are obtained. This requires a Monte Carlo simulation, followed by a stochastic model fitting. Hence, the formula (6) is computable but not computationally efficient. In section 4.2, we develop a simplified formula for t_S by numerically analyzing the full evolution of plume moments.

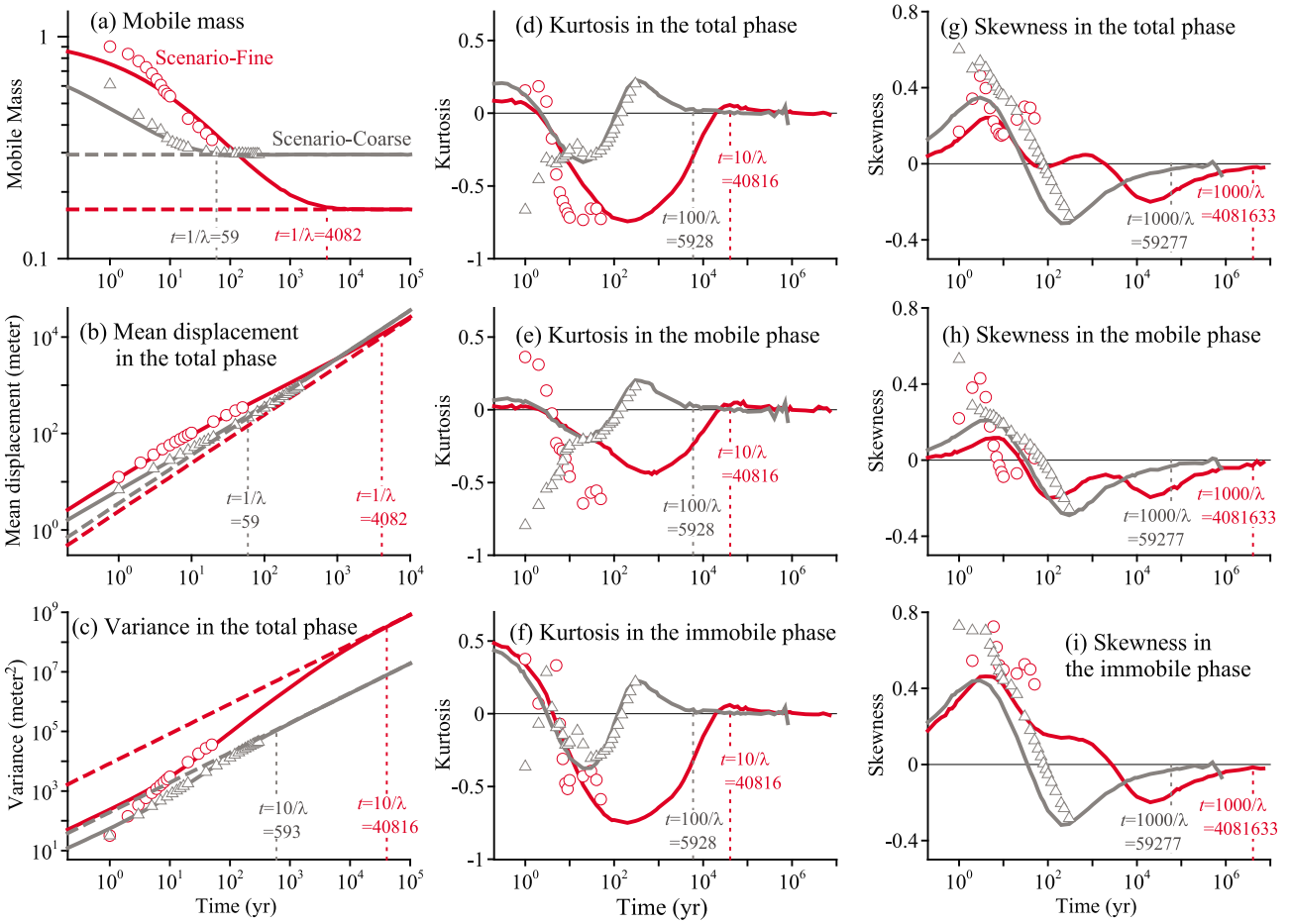

Figure 2. Evolution of spatial moments for Scenario-Fine (red) and Scenario-Coarse (grey). The symbols denote the Monte Carlo simulations, and the lines denote the prediction using the tempered stable Lévy motion (TSLM) model (1). The dashed lines in Figures 2a, 2b, and 2c denote the asymptotic moments (5), (4b), and (4c), respectively. The vertical dashed lines denote the time for each moment to reach Gaussian statistics.

4.2. Numerical Evaluation of Spatial Moments

[16] The complete evolution of spatial moments is solved numerically by a Lagrangian approach [*Meerschaert et al.*, 2008]. Monte Carlo simulations provide "real" moment data (shown by symbols in Figure 2) at early time, before particles exit the downstream boundary of the domain (see Figures 1c and 1d) used in the Monte Carlo simulation. Plume moments are ensemble averaged, to be consistent with the stochastic model. Monte Carlo simulations for Scenario-Coarse already indicate that the plume is becoming asymptotic: the mobile mass stabilizes, while the mean and variance become linear with time. The predicted moments using model (1) and parameters obtained in section 3 generally match the Monte Carlo simulations, except for very early time ($t < 3$ years; see Figure 2f) when solute particles have encountered only a small subset of the aquifer heterogeneity.

[17] Each spatial moment converges to its asymptotic limit at a different speed. Mobile mass and mean displacement converge relatively early ($t \approx 1/\lambda$, Figures 2a and 2b). The variance reaches its asymptotic limit around time $t \approx 10/\lambda$ (Figure 2c). The kurtosis approaches zero at a later time $10/\lambda \le t \le 100/\lambda$ (Figures 2d–2f), and the skewness approaches zero much later ($t \approx 1000/\lambda$, Figures 2g–2i). Therefore, only after a fairly long time

$$t_S \approx 10^3/\lambda \approx 10^3 (Z^*)^2/D^*, \tag{7}$$

will all the moments up to fourth order exhibit Gaussian statistics. Equation (7) represents a useful and practical estimate for Gaussian setting time based on matching moments, which can be computed from driller's logs.

[18] Formula (7) refines (3), showing that the setting time t_S required to match the first four moments exceeds the diffusion time scale $1/\lambda$ by three orders of magnitude. This long empirical setting time is caused by the persistence of non-Gaussian plume shape because of the "sequestration" effect [*LaBolle and Fogg*, 2001] of solute in low-permeability regions. The diffusion time scale represents the average residence time in the thickest immobile phase. By this time, the particles leaving and reentering the mobile phase approach equilibrium, resulting in a stable mass partition for particles in different phases, and Fickian scaling of the plume mean. However, the overall plume shape remains non-Gaussian for an extended period because of the sequestration effect.

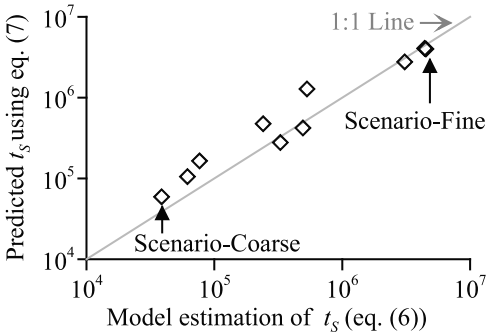

Figure 3. The predicted setting time t_S using (7) versus the estimated t_S using (6). The unit is years.

[19] Formula (7) provides a reasonable approximation to (6) for a number of simulated scenarios (Figure 3). Although the two formulae use different parameters, some parameters used in (6) can be related to the parameters in (7). For example, *Zhang et al.* [2007] found that the time index γ in (6) depends on thickness of floodplain layers. The capacity coefficient β relates to the mass partition between mobile and immobile phases (see (5)), which depends on $P(Z)$ and D^*. The velocity V, which is present in (6) but not in (7), disappears in the useful approximation $t_S \approx (-b/a)(56.25^2)$ obtained from (6) using the approximation $0 \approx D/V^2 \ll |b|$.

5. Discussion

[20] This paper has developed a useful formula (7) to predict Gaussian setting time t_S for transport in regional-scale fluvial depositional systems. The setting time can be predicted on the basis of driller's logs. Hence it can provide a useful guide to model selection. In particular, if the travel time required for the plume to settle into an asymptotic Gaussian shape exceeds the time for the plume to exit the region, then a more sophisticated preasymptotic model is indicated. In the regional-scale fluvial systems simulated in this study, the setting time t_S depends on the thickness of floodplain layers, and the rate of molecular diffusion. Thus, vertical borehole data can provide critical information for setting time because the relatively low permeability deposits tend to elongate horizontally, forcing the trapped particles to escape vertically by diffusion. The setting time formula (7) was developed on the basis of Monte Carlo simulations and extended in time using a well-tested analytic model that captures the preasymptotic behavior. The formula (7) indicates the time required for plume spatial moments (up to order 4) to approach their asymptotic values. By this time, the mobilemass, mean, variance, skewness, and kurtosis of the plume match the Gaussian ergodic limit.

[21] Previous research, using a matrix diffusion approach [e.g., *Harvey and Gorelick*, 1995; *Haggerty and Gorelick*, 1995; *Carrera et al.*, 1998; *Haggerty et al.*, 2000], suggests that the characteristic time scale for the transport behavior to become Fickian is the diffusion scale $t = 1/\lambda$ [see also *Attinger et al.*, 1999; *Kitanidis*, 1988; *Taylor*, 1954]. The matrix diffusion model is characterized by a 1/2 slope for the memory function and 3/2 slope for the BTC (point source), consistent with the parameter $\gamma = 0.53$ fitted for Scenario-Fine, and the BTC slope in Figure 1e for $D^\star = 5.2 \times 10^{-5}$ m^2/d. It would be interesting to repeat the analysis of section 3 using a matrix diffusion model, which would eliminate one fitting parameter.

[22] The Gaussian setting time t_S is found to be generally much longer than the diffusion scale $t = 1/\lambda$. This reflects the fact that plume skewness and kurtosis converge much more slowly than the variance. If the modeler wishes only to match the plume variance, the diffusion time scale may be adequate. On the other hand, even convergence of four moments is not sufficient to prove a Gaussian limit. In this sense, formula (7) may be considered optimistic. For a highly heterogeneous aquifer (e.g., Scenario-Fine) with large immobile zones (clayey lenses), the Gaussian setting time t_S is much longer than the travel time required to exit the region. The plume moves on to a different region and remains preasymptotic.

[23] The two scenarios reported here represent end-members of fluvial systems. We also checked the approximation (7) by building many additional hydrofacies models with different $P(Z)$. The predicted setting time (7) generally captured the "real" transition time to Gaussian diffusion and remained close to (6); see Figure 3 for a representative sample. The formula (7) was found accurate for lognormal K distributions, with long-range-dependent (fractal) correlations. On the other hand, our results are quite sensitive to the injection mode. A widely distributed source in the mobile zone was found to accelerate convergence to Gaussian shape. Distributing solute uniformly throughout a wide band, including mobile and immobile zones, delays the converge to an asymptotic Gaussian limit. We attribute this to particles that start out deeply embedded in an immobile zone. We conclude that the empirical setting time formula (7) may be useful to predict setting time in fluvial aquifers similar to those considered in this study, with a point source.

[24] **Acknowledgments.** Y.Z. was supported by the National Science Foundation (NSF) under grant DMS-1025417 and by the Desert Research Institute. M.M.M. was partially supported by NSF grants DMS-1025486, DMS-0803360, and EAR-0823965 and National Institutes of Health grant R01-EB012079-01. This paper does not necessarily reflect the view of the funding agencies.

References

Attinger, S., M. Dentz, H. Kinzelbach, and W. Kinzelbach (1999), Temporal behavior of a solute cloud in a chemically heterogeneous porous medium, *J. Fluid Mech.*, *386*, 77–104.

Bijeljic, B., and M. J. Blunt (2006), Pore-scale modeling and continuous time random walk analysis of dispersion in porous media, *Water Resour. Res.*, *42*, W01202, doi:10.1029/2005WR004578.

Carle, S. F., and G. E. Fogg (1996), Transition probability-based indicator geostatistics, *Math. Geol.*, *28*(4), 453–476.

Carrera, J., X. Sánchez-Vila, I. Benet, A. Medina, G. Galarza, and J. Guimerà (1998), On matrix diffusion: Formulations, solution methods and qualitative effects, *Hydrogeol. J.*, *6*(1), 178–190.

Cvetkovic, V., and R. Haggerty (2002), Transport with exchange in disordered media, *Phys. Rev. E*, *65*, 051308, doi:10.1103/PhysRevE.65.051308.

Dagan, G., and A. Fiori (2003), Time-dependent transport in heterogeneous formations of bimodal structures: 1. The model, *Water Resour. Res.*, *39*(5), 1112, doi:10.1029/2002WR001396.

Dentz, M., A. Cortis, H. Scher, and B. Berkowitz (2004), Time behavior of solute transport in heterogeneous media: Transition from anomalous to normal transport, *Adv. Water Resour.*, *27*, 155–173.

Fiori, A., I. Janković, and G. Dagan (2003), Flow and transport in highly heterogeneous formations: 2. Semianalytical results for isotropic media, *Water Resour. Res.*, *39*(9), 1269, doi:10.1029/2002WR001719.

Haggerty, R., and S. M. Gorelick (1995), Multiple-rate mass transfer for modeling diffusion and surface reactions in media with pore-scale

heterogeneity, *Water Resour. Res.*, *31*(10), 2383–2400, doi:10.1029/95WR10583.

Haggerty, R., S. A. McKenna, and L. C. Meigs (2000), On the late-time behavior of tracer test breakthrough curves, *Water Resour. Res.*, *36*(12), 3467–3479, doi:10.1029/2000WR900214.

Harvey, C., and S. M. Gorelick (1995), Temporal moment-generating equations: Modeling transport and mass transfer in heterogeneous aquifers, *Water Resour. Res.*, *31*(8), 1895–1911, doi:10.1029/95WR01231.

Kitanidis, P. K. (1988), Prediction by the method of moments of transport in a heterogeneous formation, *J. Hydrol.*, *102*, 453–473.

LaBolle, E. M. (2006), RWHet: Random walk particle model for simulating transport in heterogeneous permeable media, User's manual and program documentation, Univ. of Calif., Davis.

LaBolle, E. M., and G. E. Fogg (2001), Role of molecular diffusion in contaminant migration and recovery in an alluvial aquifer system, *Transp. Porous Media*, *42*, 155–179.

Meerschaert, M. M., Y. Zhang, and B. Baeumer (2008), Tempered anomalous diffusion in heterogeneous systems, *Geophys. Res. Lett.*, *35*, L17403, doi:10.1029/2008GL034899.

Taylor, G. I. (1954), The dispersion of matter in turbulent flow through a pipe, *Proc. R. Soc. London, Ser. A*, *223*, 446–468.

Willmann, M., J. Carrera, and X. Sánchez-Vila (2008), Transport upscaling in heterogeneous aquifers: What physical parameters control memory functions?, *Water Resour. Res.*, *44*, W12437, doi:10.1029/2007WR006531.

Zhang, Y., D. A. Benson, and B. Baeumer (2007), Predicting the tails of breakthrough curves in regional-scale alluvial systems, *Ground Water*, *45*(4), 473–484.

M. M. Meerschaert, Department of Statistics and Probability, A416 Wells Hall, Michigan State University, East Lansing, MI 48824, USA. (mcubed@stt.msu.edu)

Y. Zhang, Division of Hydrologic Sciences, Desert Research Institute, 755 E. Flamingo Rd., Las Vegas, NV 89119, USA. (yong.zhang@dri.edu)